

This is a postprint version of the following published document:

Kinvi-Dossou, G., Matadi Boumbimba, R., Bonfoh, N., Garzon-Hernandez, S., Garcia-Gonzalez, D., Gerard, P. & Arias, A. (2019). Innovative acrylic thermoplastic composites versus conventional composites: Improving the impact performances. *Composite Structures*, vol. 217, pp. 1–13.

DOI: [10.1016/j.compstruct.2019.02.090](https://doi.org/10.1016/j.compstruct.2019.02.090)

© 2019 Elsevier Ltd.



This work is licensed under a [Creative Commons Attribution-NonCommercial-NoDerivatives 4.0 International License](https://creativecommons.org/licenses/by-nc-nd/4.0/).

Innovative acrylic thermoplastic composites versus conventional composites: improving the impact performances

G. Kinvi-Dossou¹, R. Matadi Boumbimba^{1*}, N. Bonfoh¹, S. Garzon-Hernandez², D. Garcia-Gonzalez^{2,3}, P. Gerard⁴, A. Arias²

¹Université de Lorraine, CNRS, Arts et Métiers ParisTech, LEM3, F-57000 Metz, France*

²Department of Continuum Mechanics and Structural Analysis, University Carlos III of Madrid, Avenida de la Universidad 30, Leganés, 28911 Madrid, Spain

³ Department of Engineering Science, University of Oxford, Parks Road, Oxford OXI 3PJ, UK

⁴ ARKEMA, Groupement de Recherche de Lacq, F-64170 Lacq, France

Abstract

This study focuses on the benefits to the mechanical performance against impact loading offered by glass fiber reinforced (GFR) acrylic thermoplastic polymers, based on new room temperature cure methyl-methacrylate (MMA) matrix. Glass fiber reinforcement is a common solution for a wide variety of engineering applications based on thermoset matrices. However, its use presents some disadvantages such as adequate control of manufacturing temperature, problematic recycling and low damage tolerance. In contrast, acrylic polymers presents a high potential as an alternative matrix for thermoset composites due to their superior mechanical properties, manufacturing at low temperatures and recycled possibilities. In order to compare the mechanical behavior under impact loading of acrylic thermoplastic composites versus conventional composites, Charpy impact test and low velocity impact tests are carried out. The GFR acrylic laminate composites considered are compared to conventional composites manufactured with epoxy and polyester resins in terms of impact resistance and damage evolution. This study covers an impact energy rate from 10 to 60 J and analyses the maximum load, deflection, absorbed energy and associated damage, showing a better performance of the new GFR acrylic thermoplastic polymers with respect to conventional GFR composites.

Keywords: Glass fiber, Epoxy, Polyester, Acrylic thermoplastic, Nanostrength, laminate composite, low velocity impact.

*Corresponding author: matadi.boumbimba-rodrique@univ-lorraine.fr

1 Introduction

With the growing interest of reducing the carbon content in the production of materials, there is an industrial consensus to elaborate more friendly environmental materials, such as bio-based or recyclable materials[1-4]. Regarding laminated composite materials, thermoplastic matrices have become an attractive alternative for non-recyclable thermosetting matrices, thus attracting the automotive, aerospace and naval industries. In the past decade, the use of thermoplastic laminate composites was limited because of their complex preparation when using conventional methods such as resin transfer molding, infusion and pultrusion. These problems came from the difficulties to provide thermoplastic liquid resins at ambient temperature. However, the recent introduction of acrylic matrix polymers [5, 6], as ARKEMA Elium resin [7-9], opens new possibilities for the development of laminate thermoplastic composites, with special potential in the automotive industry. Moreover, Elium matrix polymers stand out because of their polymerization at room temperature, lightweight, and high performance mechanical properties [7, 8]. Unlike unsaturated polyester, Elium resins do not contain styrene. Few literature works are dedicated to the measurement and the modelling of mechanical properties of this new class of composites materials [10, 11]. Boufaida et al.[11, 12] studied the mechanical properties of laminated glass fibers/acrylic composite in terms of mesoscopic strain field analysis by combining a spectral solver and 3D-DIC (Digital image correlation) measurements. Despite the complex geometry and strong heterogeneities, the mechanical properties of these laminates composites can be determined by using numerical periodic homogenization technique [11, 12]. Pini et al. [13] reported that composite materials prepared by infusion with Elium and Elium impact (Elium filled with acrylic block copolymers at a nanometer scale) matrices depicted an intralaminar fracture toughness much higher than the one of neat Elium resin. The dependence of the fracture toughness of such composites on crack propagation speed was observed to be slightly different from that of the relevant matrices.

In a previous study [7], the enhancement of impact resistance of an Acrylic based glass fibers laminate composite, by introducing acrylic copolymer blocks was investigated at different temperatures. The impact resistance of Elium Acrylic/glass fiber laminate composite was shown to increase when copolymers (Nanostrength) were added in the Elium matrix. The study of Bhudolia et al.[9] on the evaluation of fracture toughness of thin and thick ply Elium acrylic composite systems, showed a 30% and 70% interlaminar fracture toughness for thin ply/ liquid MMA composite, compared to thick ply/liquid MMA and thin ply/epoxy composites respectively. This effect was attributed to both strong fibers-matrix interfaces and to the plastic deformation of the matrix. Strong adhesion between fibers and matrix of the aforementioned composites is essential to avoid a severe loss of mechanical properties along the thickness direction. In their applications, the glass fiber reinforced (GFR) polymers are usually subjected to impact loading during their useful life and the subsequent damage is a serious concern for the structural integrity of these components [14, 15]. In this regard, the mechanical impact process is a complex problem that includes dynamic behavior, fracture, damage, contact and friction [16-18]. Moreover, for polymer composites, damage during impact events also involves matrix cracking, fiber/matrix debonding, delamination, inter-laminar failure and fiber breakage [19, 20]. In addition, the failure evolution depends on the resin type, fiber reinforcement, orientation and thickness.

To date and for the best of the authors' knowledge, the impact behavior of GFR acrylic composites and its comparison with thermosetting based laminate composites has not been addressed against low velocity impact. The present work aims at comparing the impact resistance of Acrylic, Epoxy and Polyester based glass fibers laminate composites under low impact velocity conditions, covering an energy impact range from 10J to 60 J. To this end, an analysis of the impact performance in terms of maximum load, deflection, energy and damage evolution is conducted. The addition of copolymers to the acrylic resin leads to further

improvement of its resistance to impact, which is explained by the strong interfacial adhesion between glass fiber and matrix as well as by the positive strain rate of matrix polymer.

2 Materials and methods

This section presents a brief description of the materials tested as well as a detailed description of the experimental setups used in this work.

2.1 Materials

In this work, the mechanical performance against impact loading of GFR acrylic laminate composites are studied and compared to composites manufactured with epoxy and polyester resins. In addition, different acrylic matrices filled with shock modifiers are also prepared to study the improvement of mechanical performance against impact loads. The liquid thermoplastic acrylic resin (Elium) was supplied by Arkema (GRL, France). This liquid thermoplastic acrylic resin (ELIUM 150) with a low viscosity (150cp) is used to manufacture glass fiber reinforced composites. In addition to the acrylic monomer, this resin contains a peroxide catalyst to initiate the polymerization and an accelerator agent aimed at activating the peroxide catalyst. The hardener, supplied by Axson Technologies, is used in a ratio of 0.345 w/w (corresponding to 34.5 g of hardener for 100 g of resin). The fibers fabric used, with a repeating length unit of $T=7.8$ mm, is a plain bi-directional woven fabric glass fibers, with a thickness of 0.15 mm and surface density of 600 g/ m². This woven glass fibers fabric was provided by Chomarat. For the preparation of laminates composites containing shock modifiers, two types of copolymers are used. The first one is the acrylic tri-block copolymers M52N, named Nanostrength and supplied by ARKEMA (GRL, France), as a symmetric functionalized MAM copolymer. MAM copolymers have a poly (butyl acrylate) center block and two poly (methyl methacrylate) side blocks. The second one is the Acrylonitrile butadiene styrene (ABS). Achieved by copolymerization of styrene, butadiene and acrylonitrile, ABS consists of two essential elements: a copolymer of acrylonitrile / styrene (SAN), which constitutes the matrix,

and rubber nodules. On the other hand, the epoxy resin used is a low viscosity epoxy and its precursor is "diglycidyl ether of bisphenol A": DGEBA (EPOLAM2020). The polyester resin used is a pre-accelerated synolite having a good level of polymerization. Our composite panel is composed of four plies of woven glass fabrics. The ratio of glass fibers to resin is kept constant and equals 65% by weight. All the details about the materials and manufacturing processes are reported elsewhere [7] and summarized in Table 1.

2.2 Methods

In this paper, the impact behavior of glass fiber reinforced (GFR) acrylic thermoplastic polymers based on a new room temperature cure methyl-methacrylate (MMA) matrix is analyzed. For that, a series of Charpy impact tests and drop-weight impact tests are carried out.

2.2.1 Charpy impact tests

Charpy test (see Fig.1) permits evaluating fracture toughness. Although it was originally developed for metal, lately it has been extended to determine the fracture toughness of composite materials. In this work, Charpy tests are performed on neat and composite laminate samples by using notched samples with dimensions of 60x12x2 mm and notch length of 2 mm. The impact strength properties are determined on neat and composite laminate samples.

2.2.2 Low velocity impact tests

A series of low velocity impact tests are carried out on an Instron drop weight tower (see Fig.2) covering impact energy range from 10 to 60J at ambient temperature (20°C). The tests are performed following the ASTM D7136. For that, composites plates (100 ×150 mm) with a thickness of 2 mm are fixed on a fixture plate clamped using four rubber-tipped clamps. A steel hemispherical striker used, whose larger diameter is 16 mm and mass of about 0.1255 kg. The striker is attached to the instrumented bar attached to a metal bar, with a total mass of 5.419 kg. The drop tower device is equipped with a photocell accelerometer able to measure the impactor speed just before the contact between the impactor and the composite laminate plate and to

engage the anti-rebound system in order to prevent multiple impacts. A high-speed video camera (Photron Ultima APX-RS) placed perpendicular to the impact direction is used to measure the impactor displacement. The camera is configured to obtain 20000 frames per second (fps). In addition, two 1200 W HMI lamps are used to adequate the lighting. Moreover, with the aim to analyze the damage evolution during the impact process, a mirror is placed between the supports of the rigid base.

3 Results and discussion

This section provides the experimental observations from the different impact tests conducted and the analysis and discussion of these results.

3.1 Charpy impact tests

3.1.1 GFR acrylic composite versus conventional composites

The impact strength and resilience of the GFR acrylic composite is determined and compared with the epoxy and polyester based laminate composited Fig. 3. In addition, their corresponding matrices are also obtained. From Fig. 3a, it can be observed that, compared with neat polyester (which depicts an impact strength value of 0.6 kJ/m^2), the Epoxy and neat Elium Acrylic (E150) present an increase in impact strength of about 45 and 81.7%, respectively. This increase in impact energy is due to the ductile behavior of neat Elium acrylic. When used as a resin for the impregnation of glass fabrics, the Acrylic based laminate composite also presents the most improved impact properties compared to epoxy and polyester based laminate composites. According to the results reported in Fig. 3b and compared to polyester/GF (which depicts an impact strength value of 12.1 kJ/m^2), the Epoxy/GF and E150/GF present an increase in impact strength of about 40 and 472%, respectively. The improvement of the interfacial adhesion between glass fibers and Elium Acrylic based matrices explains the better impact strength properties obtained with these matrices.

3.1.2 GFR acrylic composite versus modified acrylic composites

The addition of copolymers in the acrylics resins presents an increase in impact resistance of 43% for the EIM150F and 235.7% for the EIM150. Moreover, this increase is also observed in the GFR composites, where the use of copolymers leads to an increase of about 8.3% for the EIM150F and 28.5% for the EIM150 compared with neat acrylic resin based laminate composite.

3.2 Low velocity impact tests

3.2.1 GFR acrylic composite versus conventional composites

3.2.1.1 Influence of impact energy

Low velocity impact tests are conducted at 20 °C and at different impact energies, from 10J to 60 J, for the composites reported in Table 1. Each test condition is repeated three times in order to ensure the repeatability of the results. Load versus displacement curves of glass fibers/epoxy, polyester and Acrylic laminate composites for an impact energy of 10 J are shown in Fig. 4. As observed for these loading conditions, the three composites present the same trends of load-versus displacement curves. An increase of load until reaching the maximum value is observed as a consequence of elastic bending of the plate. This stage is followed by a decrease of load due to the return of the impactor. As revealed by those results, the dynamic modulus, which corresponds to the slope of load versus displacement curves, is greater for laminated composite with Elium Acrylic resin, compared to the ones with both epoxy and polyester. In contrast, the displacement corresponding to the maximum load seems to be greater for epoxy and polyester based laminate composites, Fig. 5a.

At 20 J, Fig 5b, the impact behavior trend is still the same for Elium Acrylic based composite, showing no severe damage in the composite plate. However, after a monotonic load increase,

both Epoxy and polyester based laminate show an abrupt decrease of load before the return of the impactor. In addition, the Elium Acrylic based composite also presents the most significant maximum load value among all the composites. Both epoxy and polyester composites present more damage, essentially in the form of delamination, see Fig. 6 for the corresponding evolution of force and energy with time. In this regard, when comparing the absorbed energy of the three GFR composites, corresponding to the plateau value of energy versus time, the Elium acrylic based composite shows a value of around 12.7 J. In contrast, both polyester and epoxy-based composites present absorbed energy values of 17.5 and 17.6 J, respectively, which is closer to the incident energy. Thus, a great part of incident energy in this case is used to generate damage in epoxy and polyester based composites. That damage is essentially in the form of matrix cracking and delamination. However, for this impact energy, no perforation occurs since the absorbed energy is still lower than the incident energy.

In Fig. 7, the load versus displacement curves of all the laminate composites for impact energies from 30 to 60 J is reported. Conventional composites, as the considered epoxy and polyester based composites, still present an abrupt decrease of the load after reaching the maximum load value. This stage is followed by a new slight increase of the load, which occurs with oscillations. This decrease is due to the perforation of the first laminate composite layers and the propagation of the delamination at the interface between layers, as revealed by the post mortem observations, Fig. 8. As revealed by several authors, this significant drop could correspond to the loss of contact between the impactor and the plate [7, 21]. In other words, when the projectile impacts the front face of the plate, some near layers might be suddenly subjected to a large delamination, leading to the loss of contact between the plate and the impactor [7]. Once the impactor crosses the space left by layers' dissociation, it impacts the remaining layers causing the load rise before the return of the impactor. This behavior is particularly noticeable in sandwich structures

subjected to impact loading. Indeed, for these latter structures, the drastic load drop is caused by the loss of bonding area between the sheet and the core, but also by the core low stiffness. This particular response occurs in the case of both epoxy and polyester because of their low toughness properties, which facilitate the apparition of matrix cracking and severe delamination [22, 23]. In terms of absorbed energy, Fig. 9, both materials absorb too much energy, with a slight increase in the case of polyester based composite compared to the epoxy based one. However, no penetration occurs for all the materials, since, as mention previously, the absorbed energy is still lower than the incident energy.

Figs. 7 and 9 also reveal in an obvious way the most enhanced impact properties of the Elium acrylic resin based composite with respect to epoxy and polyester. In fact, when the impact energy increases, the Elium acrylic based laminate globally maintains the same trends in terms of load versus displacement curve, elastic bending of the plate with occurrence of small oscillations (corresponding to the onset of damage, essentially in the form of matrix cracking), before reaching the maximum load and the return of the impactor. There is no abrupt decrease of the load, revealing the limitation of the damage evolution as shown in Fig. 10. In terms of absorbed energy, the Elium Acrylic resin presents lower values compared to epoxy and polyester based composite. In this specific case, around 10 J of elastic energy is always returned to the impactor. The Elium Acrylic based composite also presents the most significant maximum load. When increasing the impact energy, this maximum value increases confirming the strain rate dependency of this composite.

3.2.1.2 Post mortem observations and damage evolution

For all the impact energies tested, Fig. 8, the Elium acrylic based laminate presents less damage with respect to epoxy and polyester composites. According to the post-mortem observations, the polyester composite presents a larger delamination zone compared to the other composites.

For all the composites, when the impact energy increases, matrix cracks in form of shear failure mode propagate radially from the top down, inclined at about $\pm 45^\circ$ from the vertical position. A more significant damage is observed for the two thermoset based laminate composites compared with Elium acrylic composite, explained by their lower toughness. Previous results are consistent with the post mortem observations.

The evolution of the damage during the impact process is analyzed for different impact energies, Figs. 10, 11 and 12. In Fig. 10, different stages of the damage process can be observed for the Epoxy/GF, polyester/GF and E150/GF impacted at an impact energy of 10 J. A progressive damage growth is observed for the three composites materials until reaching the maximum load value ($t=6.05$ ms). In the three cases, local damage due to matrix cracking is observed in the impact zone, being the polyester based composites the ones presenting greater damage. At an impact energy of 20 J, a delamination zone can be observed for polyester and epoxy composites. This delamination damage grows from the edge of the specimen to the center, and is associated with the boundary conditions used in this work. While the initiation of the delamination process in the polyester composite is observed before reaching the maximum load value ($t=5$ ms), for the epoxy composite the delamination process starts after reaching the maximum load value, Fig. 10. These observations agree with the results presented in Fig. 5. When the impact energy increases, matrix cracks propagation is observed at $\pm 45^\circ$ for all the cases, Fig. 11. In all the cases, greater damage is observed for the polyester and epoxy composites due to their lower toughness compared with Elium acrylic composite.

As demonstrated by Bhudolia et al.[9], the improvement of the impact properties of Elium acrylic based laminated composite is attributed to the better fiber/matrix interfaces. The damage propagation in the Elium acrylic laminate composite seems to be generated by the matrix cracking, with a relatively lower failure of fibers-matrix interfaces, explaining why this composite exhibits a higher dynamic modulus compared to Epoxy and Polyester based

composite. The higher fracture toughness of Elium acrylic based composite plays a major role in improving the crack propagation within the laminate. This fact may be explained by the plastic deformation of the matrix with the subsequent increase in ductility. As reported by some authors, any mechanism that facilitates the shear localization process, or alternatively dissipates the bulk strain energy, would enhance the toughness [24, 25]. The Elium Acrylic based laminate seems to do both by increasing the matrix shear banding. In contrast, for the polyester and epoxy based laminate composite the great crosslinking density leads to very brittle materials, especially for polyester. When subjected to impact loading, the rapid propagation of micro-cracks generates more delamination. As mentioned previously, a great part of the incident energy is dissipated by delamination.

3.2.1.3 Penetration threshold curves and energy profile diagram

In order to measure the real improvement in impact resistance of Elium acrylic based composite, the penetration threshold curves are fitted for the three materials. In fact, it is well known that the penetration threshold is one the most important criteria, allowing for the measurement of the impact properties of laminate composites [19, 26]. This parameter determines the energy required to perforate the composite laminate. Among several criteria, we choose for the present study to use the criteria defined by Reis et al.[27] and Aktas et al.[28]. These authors defined an energy profile diagram (EPD) that is useful to compare the impact and absorbed energies, as well as to identify the penetration and perforation thresholds. According to Aktas et al.[28], the penetration threshold can be defined as the point where the absorbed energy equals the incident impact energy. The authors also define another criteria which consists to plot the elastic energy (E_e) versus impact energy (E_i). The elastic energy is calculated as the difference between the absorbed impact energy and the energy at the peak load (incident impact energy). The roots of the corresponding fitting second degree polynomial equations give energy points where impact

energy (E_i) is equal to the absorbed energy (E_a), i.e. where $E_e = 0$. The higher roots imply penetration thresholds for laminates.

Fig. 13 shows the energy profile diagram (EPD) of all the materials tested. No penetration occurs for any of the studied composites since the absorbed energies are lower than the incident impact energy. All the experimental points are found below the equal energy line, meaning that the penetration threshold is not reached in this region and, therefore, excessive energy is consumed to rebound the impactor. However, the Elium Acrylic based composite presents the highest improvement in impact properties, with all experimental data located below and far from the equal energy line.

3.2.2 GFR acrylic composite versus modified acrylic composites

3.2.2.1 Influence of impact energy

The addition of copolymers to the Elium Acrylic resin results in a decrease of both the dynamic modulus and maximum load, as observed in Figs. 14 and 15 for tests performed at 10 and 20 J. The shape of the load versus displacement curves are the same even when the copolymers are added in the Elium Acrylic resin. At 20 J, after a monotonic evolution, a slight decrease of the load is observed before reaching the ultimate value for both modified and non-modified Elium Acrylic based composites. In terms of energy versus time curves, Fig. 15, the addition of copolymers does not provide any improvement in the impact response at impact energies of 10 and 20 J. In fact, the absorbed energy presents the same value for modified and non-modified Elium acrylic laminate composites.

At 30 J, the same observations can be made, Fig. 16a. However, when the impact energy increases, the composites containing copolymers presents a better impact resistance compared to the neat Elium acrylic based composite, Figs. 16a, b and c. In this regard, their absorbed energy is found lower than the one of Elium acrylic composite, see figure 17.

3.2.2.2 Penetration threshold curves and energy profile diagram

Previous results are a consequent of the threshold penetration values (Fig. 18), where the threshold penetration increases with the addition of nano-copolymers, especially at high impact energies. The penetration thresholds, Fig. 18b, are 78 J, 82 J, and 83 J for E150/GF, EIM150/GF and EIM150/GF, respectively.

In the case of Elium Acrylic resin filled with Nanostrength and ABS, the copolymers, which containing a rubber blocs at nanometer scale, tends to make the Elium acrylic more ductile leading to more plastic deformation when subjected to low velocity impact. By making the Acrylic matrix more ductile, the Nanostrength could act to bridge cracks, by shielding the matrix from damage. Ahead of the crack front, Nanostrength is able to act within the plastic zone by suppressing coalescence of micro-cracks and voids [26]. Additionally, it is well known that in ductile materials, damage takes place mainly by cavitation. The improved impact resistance of laminate composites with Nanostrength can be explained by the Nanostrength micelle cavitation, which enhances the toughness of acrylic matrix [26, 29-31]. Under impact loading, micelle cavitation can induce matrix shear banding [32] and prevent delamination[33].

4 Conclusions

In order to show the benefit of the new Elium Acrylic resin in GFRC laminates by means of impact behavior, both Charpy impact strength and low velocity impact tests are performed. The major findings derive from the analysis of the five baseline materials (Glass fibers/Elium Acrylic laminate composites, Epoxy, polyester and Elium modified laminate composites) are summarized below:

- The impact strength of modified and non-modified Elium Acrylic neat resin is found significantly higher than that of neat epoxy and polyester. When used as a resin in glass fiber laminate composites, the Acrylic resin based composite presents the best impact

strength, with less pronounced effects compared to neat resins.

- The low velocity impact tests, performed at various impact energies, confirm this trend since the Elium Acrylic based composites present the best properties in terms of impact resistance with respect to epoxy and polyester based composites. At low energy (10 J), the dynamic modulus corresponding to the slope of load versus displacement curves is greater for laminate composite with Elium Acrylic resin, compared to both epoxy and polyester composites. When increasing the impact energy, the epoxy and polyester based composites present an abrupt decrease of the load after reaching the maximum load value. In terms of absorbed energy, a great part of the kinetic energy is used to generate delamination in epoxy and polyester based composites. This damage extension is found smaller for Acrylic based composite and mainly consists of slight fibers breakage. With the addition of copolymer, which self-assembled and forms micelliums at a nanometer scale, the penetration threshold shifts to higher values.

5 References

- [1] Boumbimba RM, Wang K, Hablot E, Bahlouli N, Ahzi S, Avérous L. Renewable biocomposites based on cellulose fibers and dimer fatty acid polyamide: Experiments and modeling of the stress–strain behavior. *Polymer Engineering & Science*. 2016;n/a-n/a.
- [2] Hablot E, Matadi R, Ahzi S, Avérous L. Renewable biocomposites of dimer fatty acid-based polyamides with cellulose fibres: Thermal, physical and mechanical properties. *Composites Science and Technology*. 2010;70:504-9.
- [3] Reulier M, Avérous L. Elaboration, morphology and properties of renewable thermoplastics blends, based on polyamide and polyurethane synthesized from dimer fatty acids. *European Polymer Journal*. 2015;67:418-27.
- [4] Reulier M, Boumbimba RM, Rasselet D, Avérous L. Renewable thermoplastic multiphase systems from dimer fatty acids, with mineral microfillers. *Journal of Applied Polymer Science*. 2016;133:n/a-n/a.
- [5] Kishi H, Nakao N, Kuwashiro S, Matsuda S. Carbon fiber reinforced thermoplastic composites from acrylic polymer matrices: Interfacial adhesion and physical properties. *Express Polymer Letters*. 2017;11:334-42.
- [6] Pini T, Caimmi F, Briatico-Vangosa F, Frassine R, Rink M. Fracture initiation and propagation in unidirectional CF composites based on thermoplastic acrylic resins. *Engineering Fracture Mechanics*. 2017;184:51-8.

- [7] Matadi Boumbimba R, Coulibaly M, Khabouchi A, Kinvi-Dossou G, Bonfoh N, Gerard P. Glass fibres reinforced acrylic thermoplastic resin-based tri-block copolymers composites: Low velocity impact response at various temperatures. *Composite Structures*. 2017;160:939-51.
- [8] Kinvi-Dossou G, Matadi Boumbimba R, Bonfoh N, Koutsawa Y, Eccli D, Gerard P. A numerical homogenization of E-glass/acrylic woven composite laminates: Application to low velocity impact. *Composite Structures*. 2018;200:540-54.
- [9] Bhudolia SK, Joshi SC. Low-velocity impact response of carbon fibre composites with novel liquid Methylmethacrylate thermoplastic matrix. *Composite Structures*. 2018;203:696-708.
- [10] Bhudolia SK, Perrotey P, Joshi SC. Mode I fracture toughness and fractographic investigation of carbon fibre composites with liquid Methylmethacrylate thermoplastic matrix. *Composites Part B: Engineering*. 2018;134:246-53.
- [11] Boufaïda Z, Farge L, André S, Meshaka Y. Influence of the fiber/matrix strength on the mechanical properties of a glass fiber/thermoplastic-matrix plain weave fabric composite. *Composites Part A: Applied Science and Manufacturing*. 2015;75:28-38.
- [12] Boufaïda Z, Boisse J, André S, Farge L. Mesoscopic strain field analysis in a woven composite using a spectral solver and 3D-DIC measurements. *Composite Structures*. 2017;160:604-12.
- [13] Pini T, Briatico-Vangosa F, Frassine R, Rink M. Time dependent fracture behaviour of a carbon fibre composite based on a (rubber toughened) acrylic polymer. *Procedia Structural Integrity*. 2016;2:253-60.
- [14] Garcia-Gonzalez D, Rodriguez-Millan M, Rusinek A, Arias A. Investigation of mechanical impact behavior of short carbon-fiber-reinforced PEEK composites. *Composite Structures*. 2015;133:1116-26.
- [15] Garcia-Gonzalez D, Rusinek A, Jankowiak T, Arias A. Mechanical impact behavior of polyether-ether-ketone (PEEK). *Composite Structures*. 2015;124:88-99.
- [16] Garcia-Gonzalez D, Zaera R, Arias A. A hyperelastic-thermoviscoplastic constitutive model for semi-crystalline polymers: Application to PEEK under dynamic loading conditions. *International Journal of Plasticity*. 2017;88:27-52.
- [17] Rodríguez-Millán M, Vaz-Romero A, Rusinek A, Rodríguez-Martínez JA, Arias A. Experimental Study on the Perforation Process of 5754-H111 and 6082-T6 Aluminium Plates Subjected to Normal Impact by Conical, Hemispherical and Blunt Projectiles. *Experimental Mechanics*. 2014;54:729-42.
- [18] Rodríguez-Martínez JA, Rusinek A, Chevrier P, Bernier R, Arias A. Temperature measurements on ES steel sheets subjected to perforation by hemispherical projectiles. *International Journal of Impact Engineering*. 2010;37:828-41.
- [19] Matadi Boumbimba R, Froustey C, Viot P, Gerard P. Low velocity impact response and damage of laminate composite glass fibre/epoxy based tri-block copolymer. *Composites Part B: Engineering*. 2015;76:332-42.
- [20] Garcia-Gonzalez D, Rodriguez-Millan M, Rusinek A, Arias A. Low temperature effect on impact energy absorption capability of PEEK composites. *Composite Structures*. 2015;134:440-9.
- [21] Ghasemi Nejjhad MN, Parvizi-Majidi A. Impact behaviour and damage tolerance of woven carbon fibre-reinforced thermoplastic composites. *Composites*. 1990;21:155-68.
- [22] Gustin J, Freeman B, Stone J, Mahinfalah M, Salehi-Khojin A. Low-velocity impact of nanocomposite and polymer plates. *Journal of Applied Polymer Science*. 2005;96:2309-15.
- [23] Ramakrishnan KR, Guérard S, Viot P, Shankar K. Effect of block copolymer nano-reinforcements on the low velocity impact response of sandwich structures. *Composite Structures*. 2014;110:174-82.

- [24] Pearson RA, Yee AF. Toughening mechanisms in elastomer-modified epoxies. *Journal of Materials Science*. 1989;24:2571-80.
- [25] Liang YL, Pearson RA. The toughening mechanism in hybrid epoxy-silica-rubber nanocomposites (HESRNs). *Polymer*. 2010;51:4880-90.
- [26] Matadi Boumbimba R, Froustey C, Viot P, Olive JM, Léonardi F, Gerard P, et al. Preparation and mechanical characterisation of laminate composites made of glass fibre/epoxy resin filled with tri bloc copolymers. *Composite Structures*. 2014;116:414-22.
- [27] Reis PNB, Ferreira JAM, Zhang ZY, Benameur T, Richardson MOW. Impact response of Kevlar composites with nanoclay enhanced epoxy matrix. *Composites Part B: Engineering*. 2013;46:7-14.
- [28] Aktaş M, Atas C, İçten BM, Karakuzu R. An experimental investigation of the impact response of composite laminates. *Composite Structures*. 2009;87:307-13.
- [29] Yang X, Yi F, Xin Z, Zheng S. Morphology and mechanical properties of nanostructured blends of epoxy resin with poly(ϵ -caprolactone)-block-poly(butadiene-co-acrylonitrile)-block-poly(ϵ -caprolactone) triblock copolymer. *Polymer*. 2009;50:4089-100.
- [30] Lalande L, Plummer CJG, Månson J-AE, Gérard P. Microdeformation mechanisms in rubber toughened PMMA and PMMA-based copolymers. *Engineering Fracture Mechanics*. 2006;73:2413-26.
- [31] Mbarek IA, Matadi Boumbimba R, Rusinek A, Voyiadjis GZ, Gerard P, Samadi-Dooki A. The dynamic behavior of poly (methyl methacrylate) based nano-rubbers subjected to impact and perforation: Experimental investigations. *Mechanics of Materials*. 2018;122:9-25.
- [32] Bashar MT, Sundararaj U, Mertiny P. Mode-I interlaminar fracture behaviour of nanoparticle modified epoxy/basalt fibre-reinforced laminates. *Polymer Testing*. 2013;32:402-12.
- [33] Van Velthem P, Ballout W, Daoust D, Sclavons M, Cordenier F, Henry E, et al. Influence of thermoplastic diffusion on morphology gradient and on delamination toughness of RTM-manufactured composites. *Composites Part A: Applied Science and Manufacturing*. 2015;72:175-83.

Figure captions:

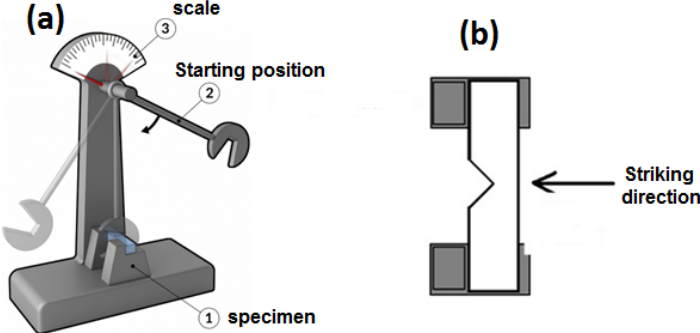


Figure 1: Schematic representation of Charpy impact tests, (a) device components, (b) clamping configuration used for Charpy tests.

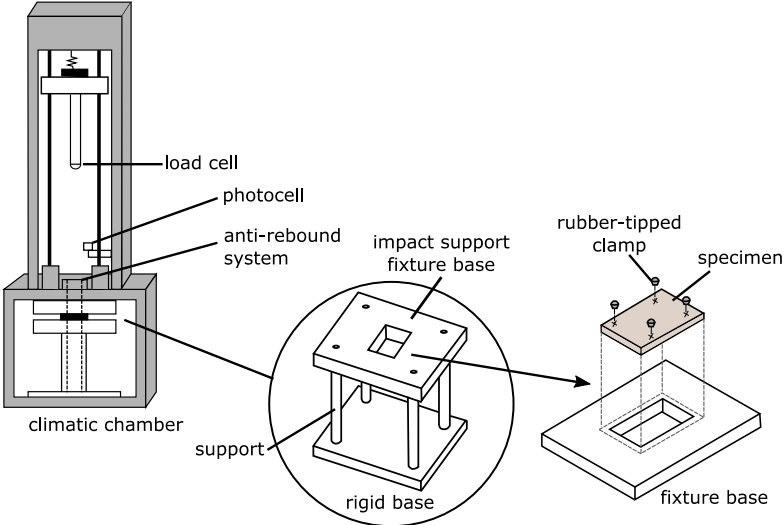


Figure 2: Experimental setup used for low velocity impact tests.

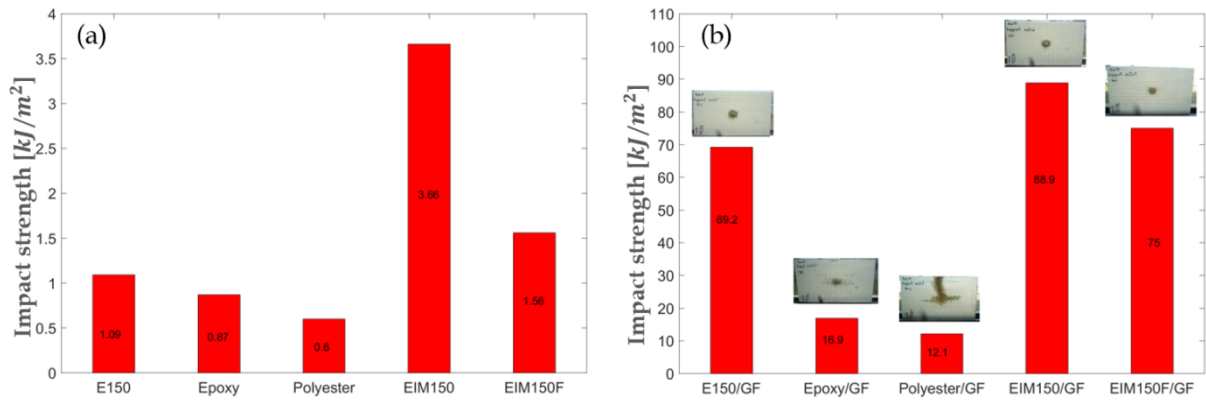


Figure 3: Impact strength obtained from Charpy impact tests: (a) neat matrix polymers; (b) composite laminates.

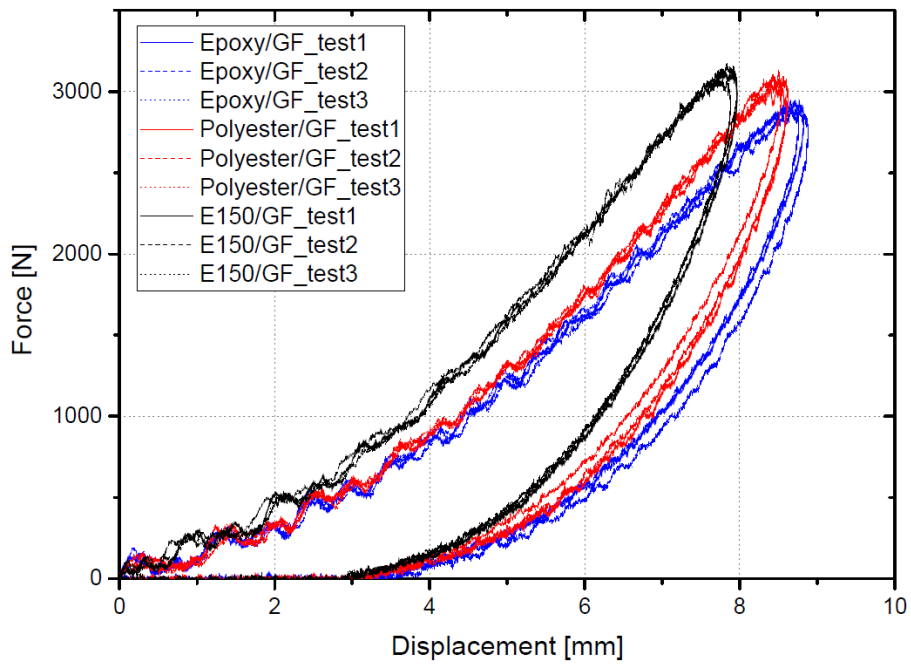


Figure 4: Force-displacement curves of GFR Epoxy, Polyester and Acrylic laminate composites at 10 J and ambient temperature, showing repeatability of the results.

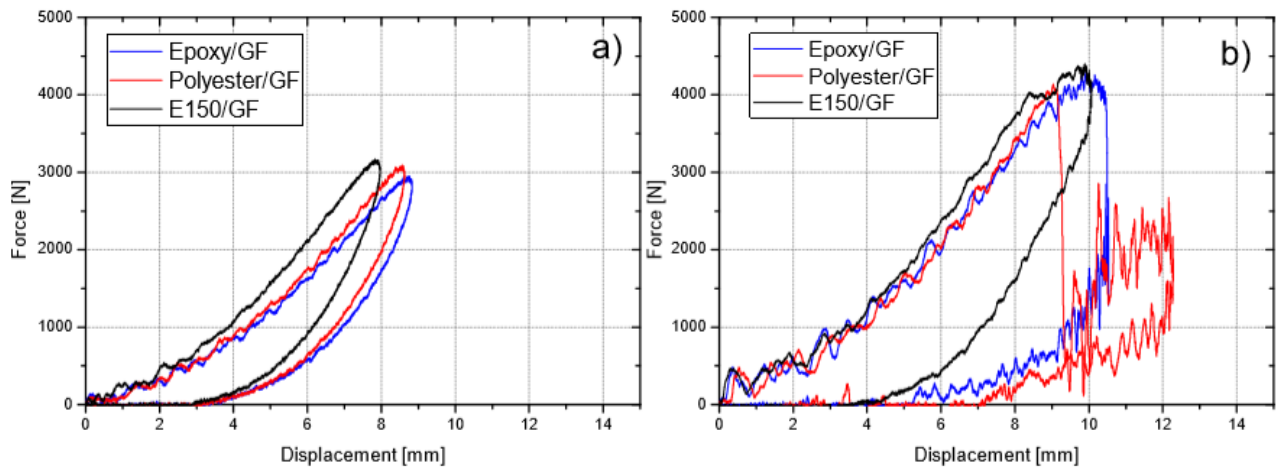


Figure 5: Force-displacement curves of GFR Epoxy, Polyester and Acrylic laminate composites: (a) 10 J impact energy; (b) 20 J impact energy.

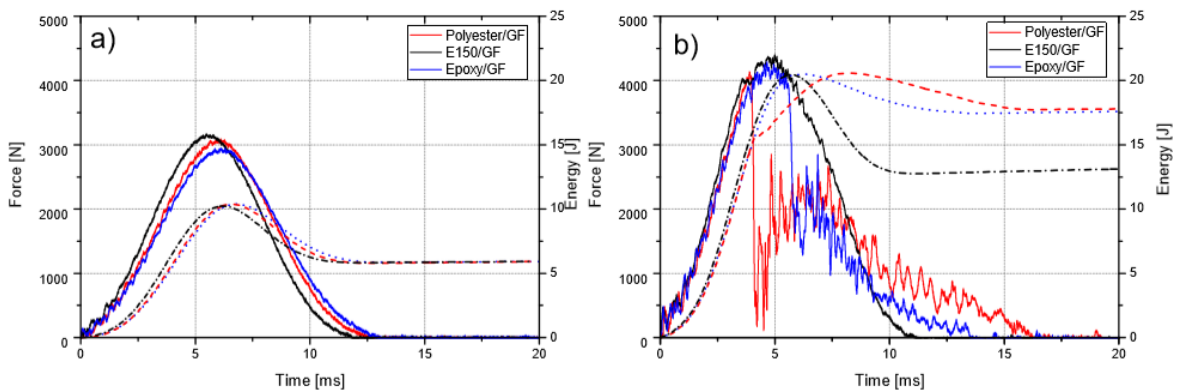


Figure 6: Force and energy versus time evolution of GFR Epoxy, Polyester and Acrylic laminate composites for impact energies of: (a) 10 J, (b) 20 J.

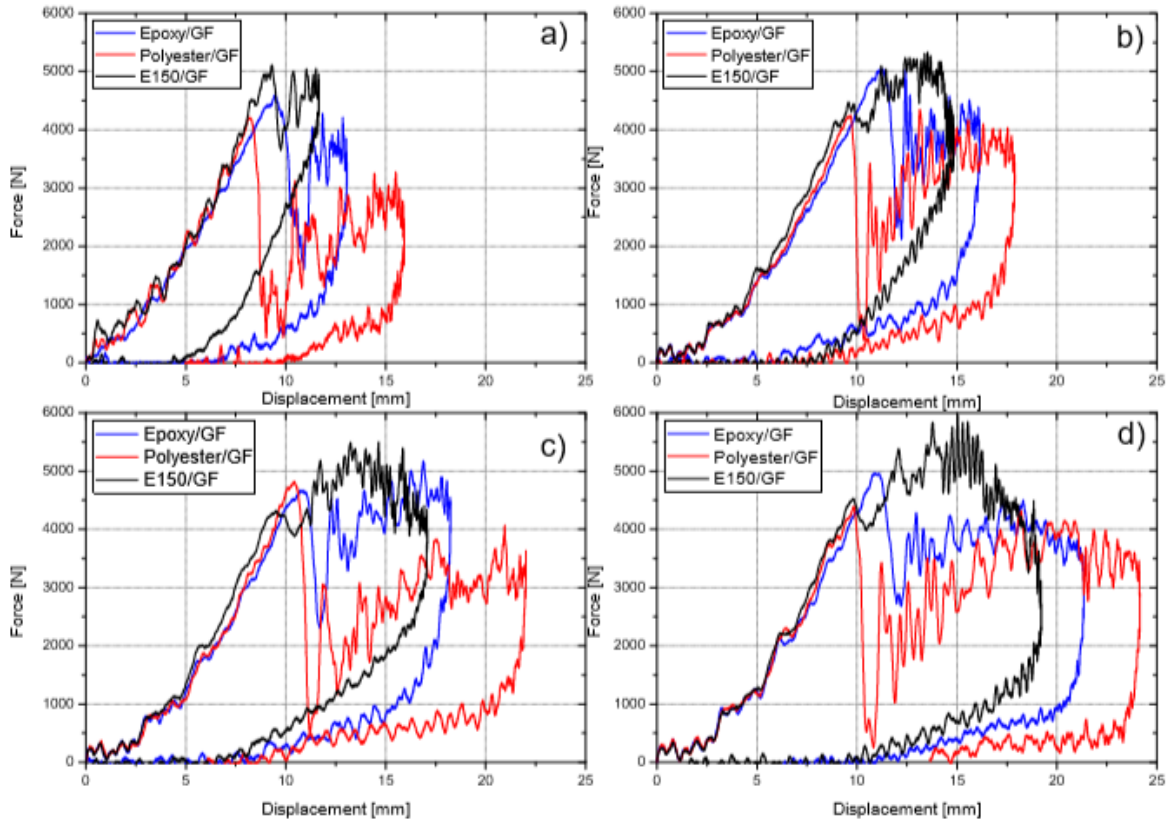


Figure 7: Force-displacement curves of GFR Epoxy, Polyester and Acrylic laminate composites for impact energies of: (a) 30 J; (b) 40 J, (c)50 J, (d) 60 J.

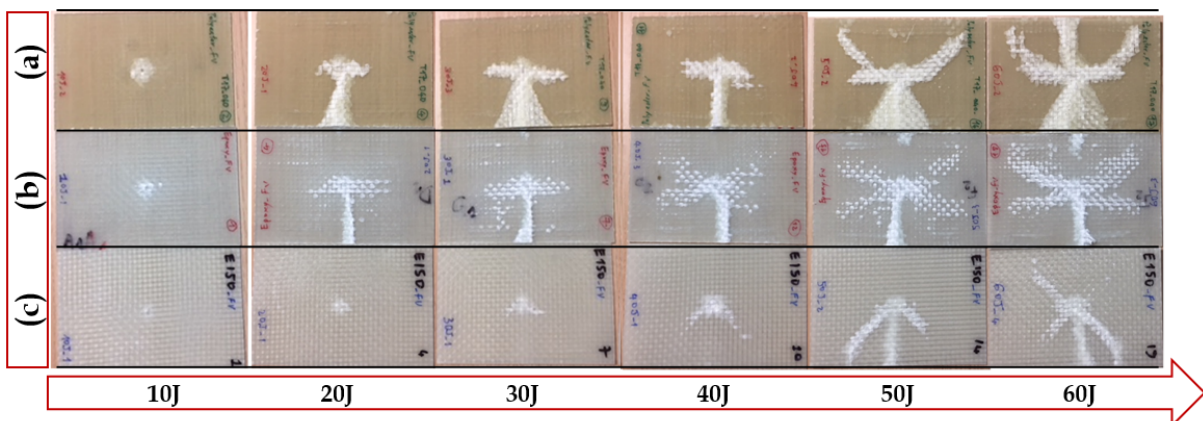


Figure 8: Final stage of damage on the front side of GFR composites: (a) Polyester; (b) Epoxy; (c) Acrylic laminate composites.

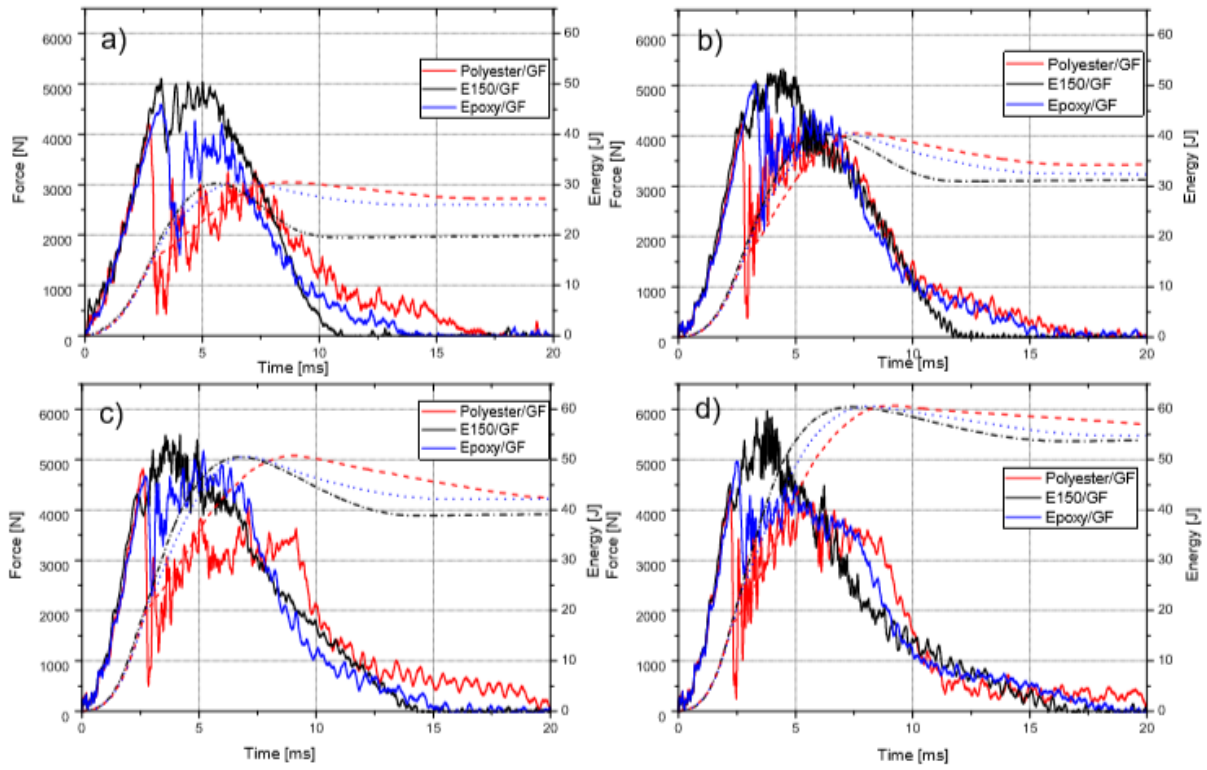


Figure 9: Force and energy evolution of GFR Epoxy, Polyester and Acrylic laminate composites for impact energies of: (a) 30 J; (b) 40 J; (c) 50; (d) 60 J.

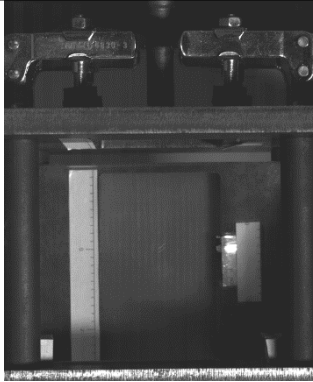
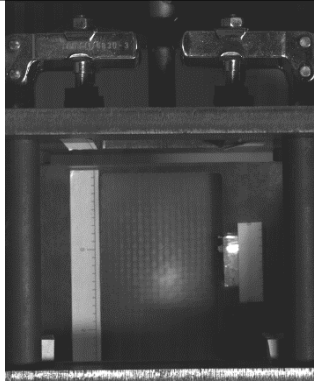
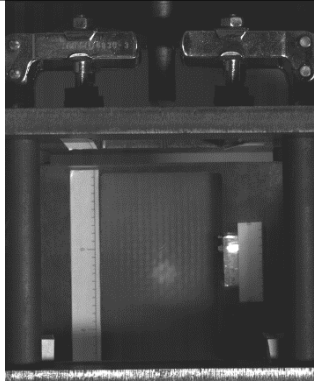
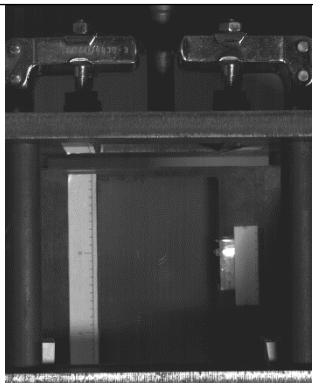
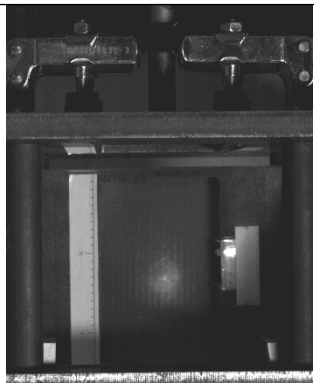
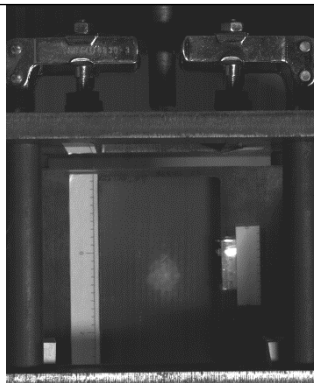
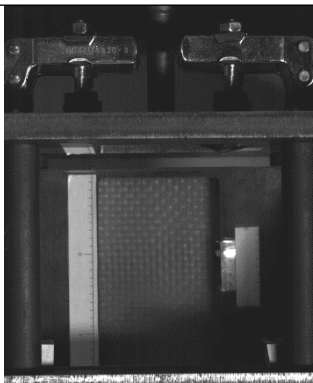
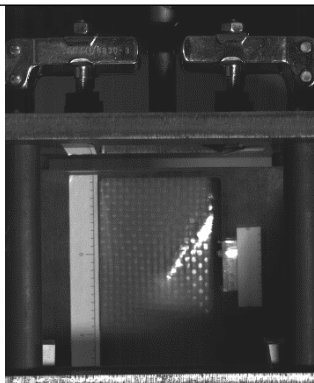
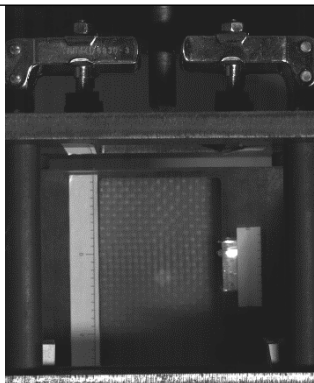
10 J			
EPOXY/GF			
	T=0 ms	T=6.05 ms	T=14.75 ms
POLYESTER/GF			
	T=0 ms	T=6.05 ms	T=14.75 ms
E150/GF			
	T=0 ms	T=6.05 ms	T=14.75 ms

Figure 10: Damage evolution of GFR composites at impact energy of 10 J.

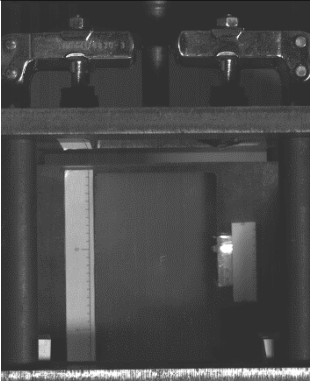
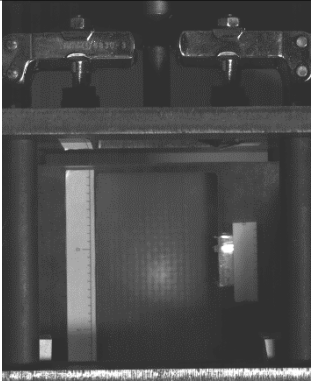
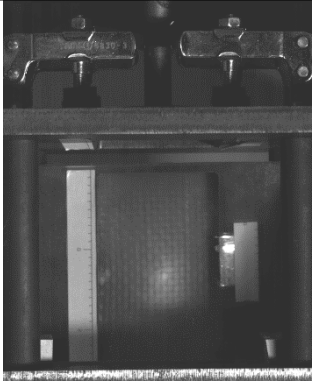
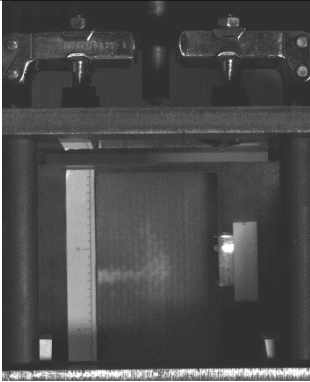
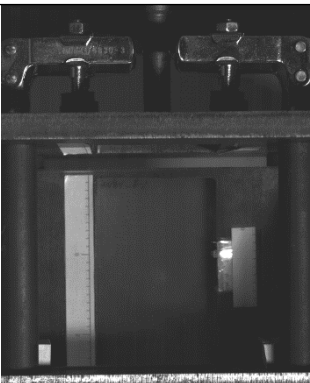
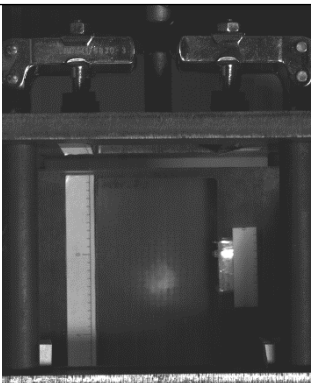
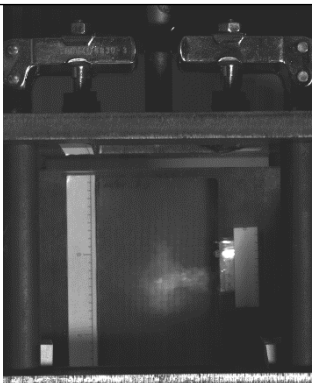
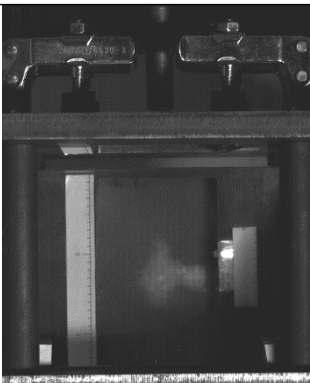
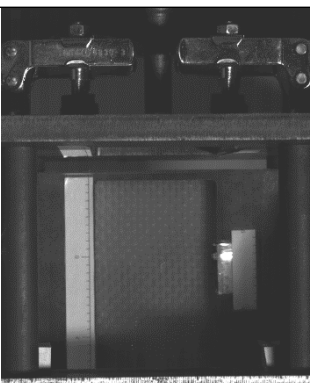
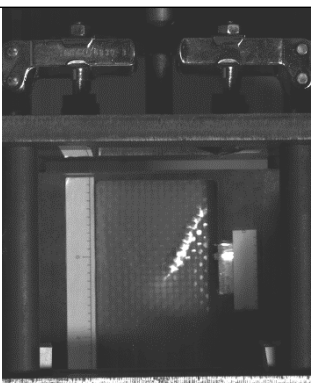
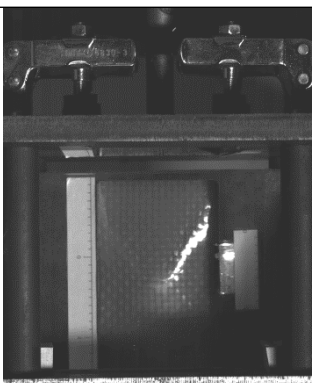
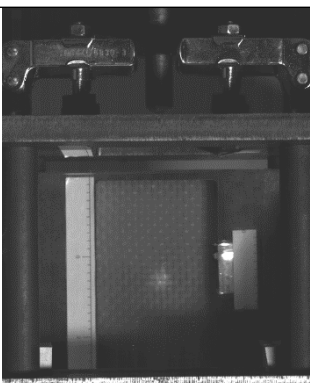
20 J				
EPOXY/GF				
	T=0 ms	T=2.5 ms	T=5 ms	T=19.4 ms
POLYESTER/GF				
	T=0 ms	T=2.5 ms	T=5 ms	T=20 ms
E150/GF				
	T=0 ms	T=2.5 ms	T=5 ms	T=14.5 ms

Figure 11: Damage evolution of GFR composites at impact energy of 20 J.

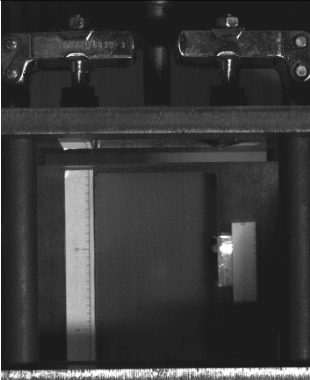
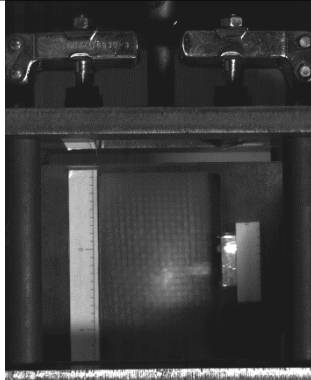
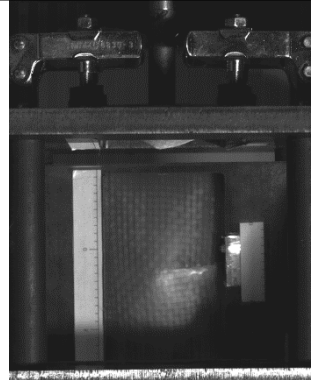
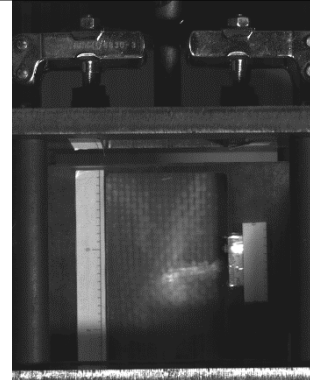
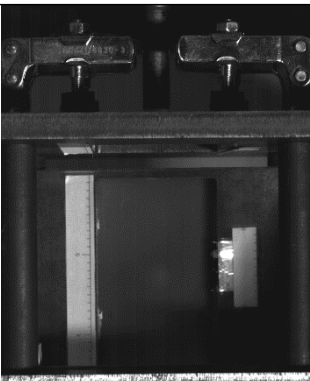
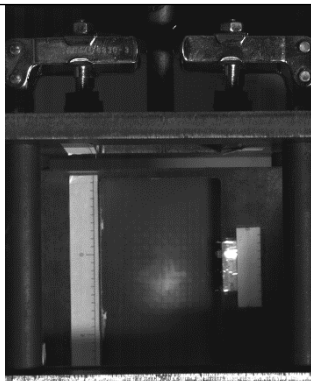
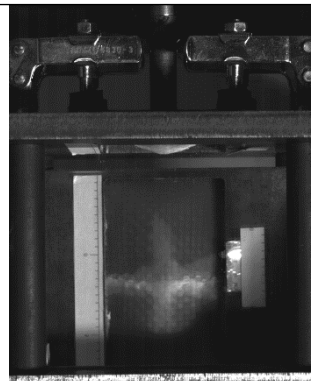
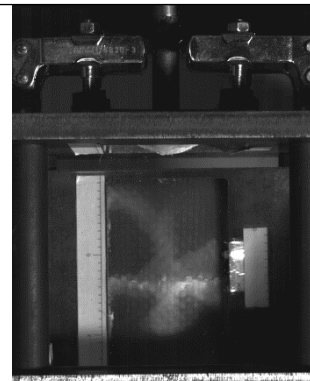
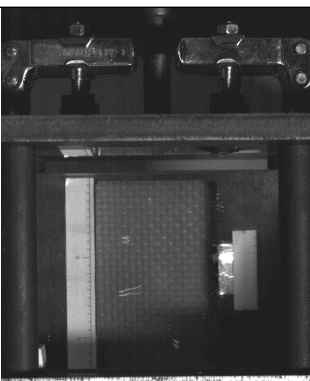
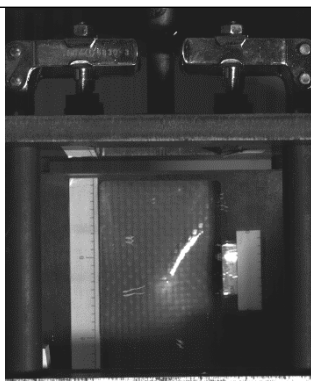
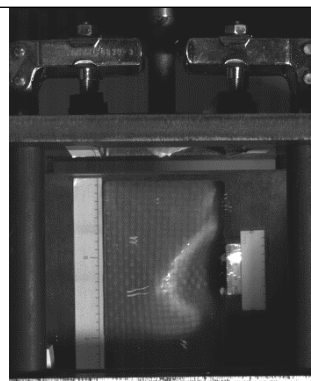
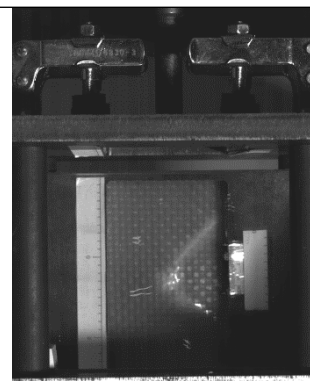
60 J				
EPOXY/GF				
	T=0 ms	T=2.5 ms	T=5 ms	T=15 ms
POLYESTER/GF				
	T=0 ms	T=2.5 ms	T=5 ms	T=15 ms
E150/GF				
	T=0 ms	T=2.5 ms	T=5 ms	T=15 ms

Figure 12: Failure stages of the impact process of GFR composites at impact energy of 60 J.

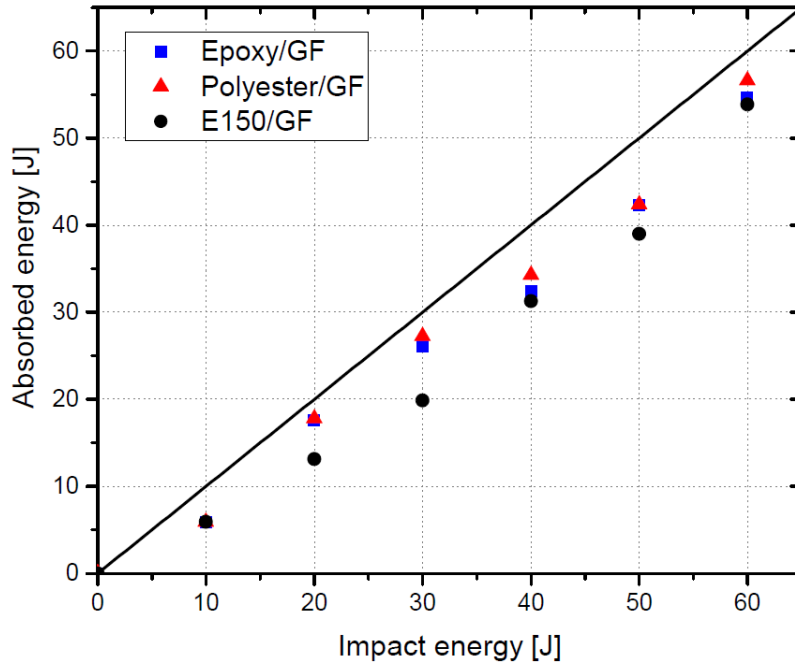


Figure 13: Penetration Threshold of glass fibres/ Epoxy, Polyester and Acrylic laminate composites, showing the improved impact properties of Acrylic based laminate composite.

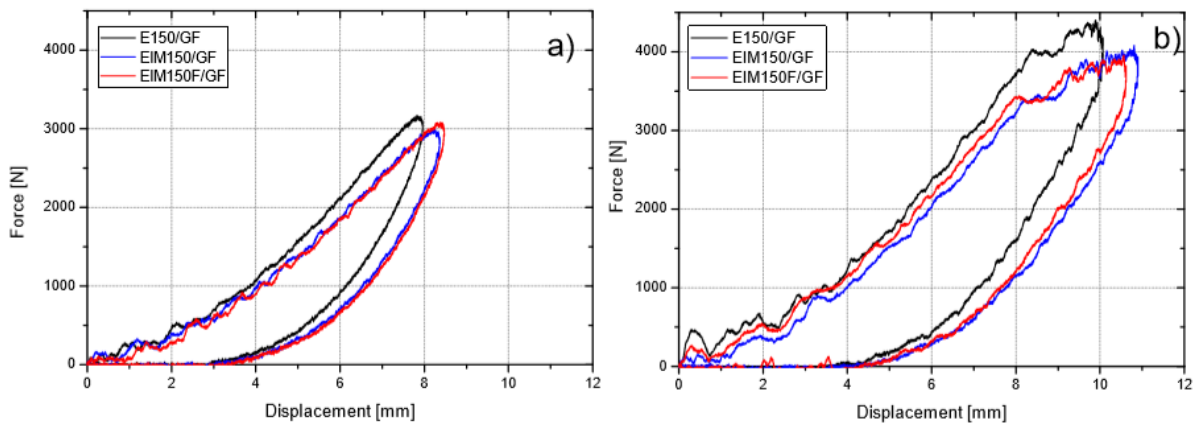


Figure 14: Effect of Acrylic copolymers on impact properties of glass fibers reinforced acrylic thermoplastic laminate composite at 20 °C, comparison with laminate obtained with neat acrylic resin: (a) test at 10 J, (b) test at 20 J.

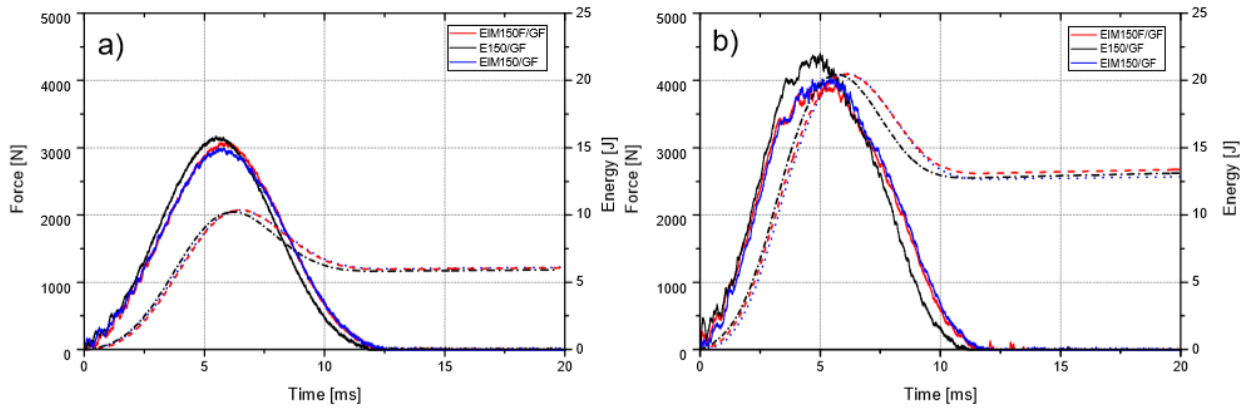


Figure 15: Force-Displacement and Energy-Time curves, showing the effect of copolymers, for impact energies of: (a) 10 J; (b) 20 J.

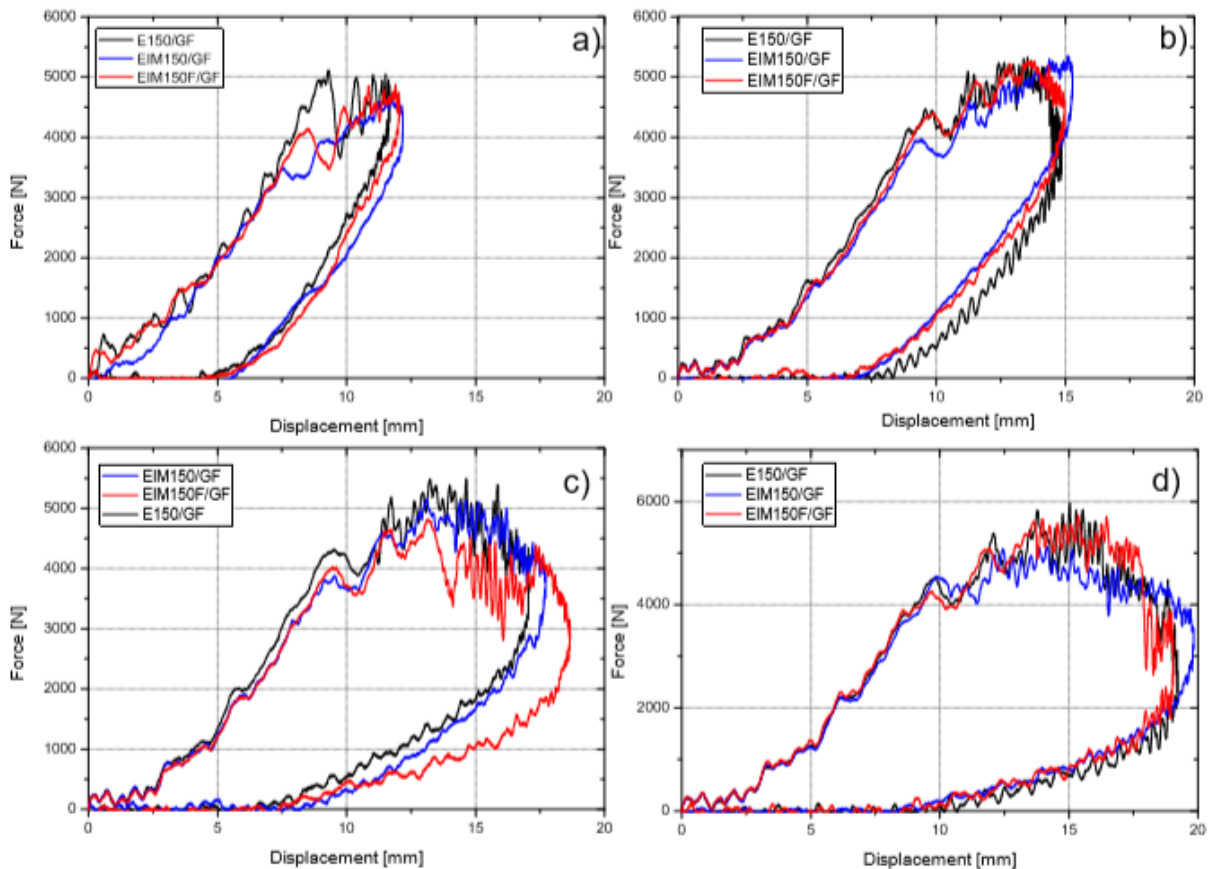


Figure 16: Effect of Acrylic copolymers on impact properties of glass fiber reinforced acrylic thermoplastic laminate composite at 20 °C, comparison with laminate obtained with neat acrylic resin: (a) test at 30 J; (b) test at 40 J; (c) test at 50 J; (d) test at 60 J.

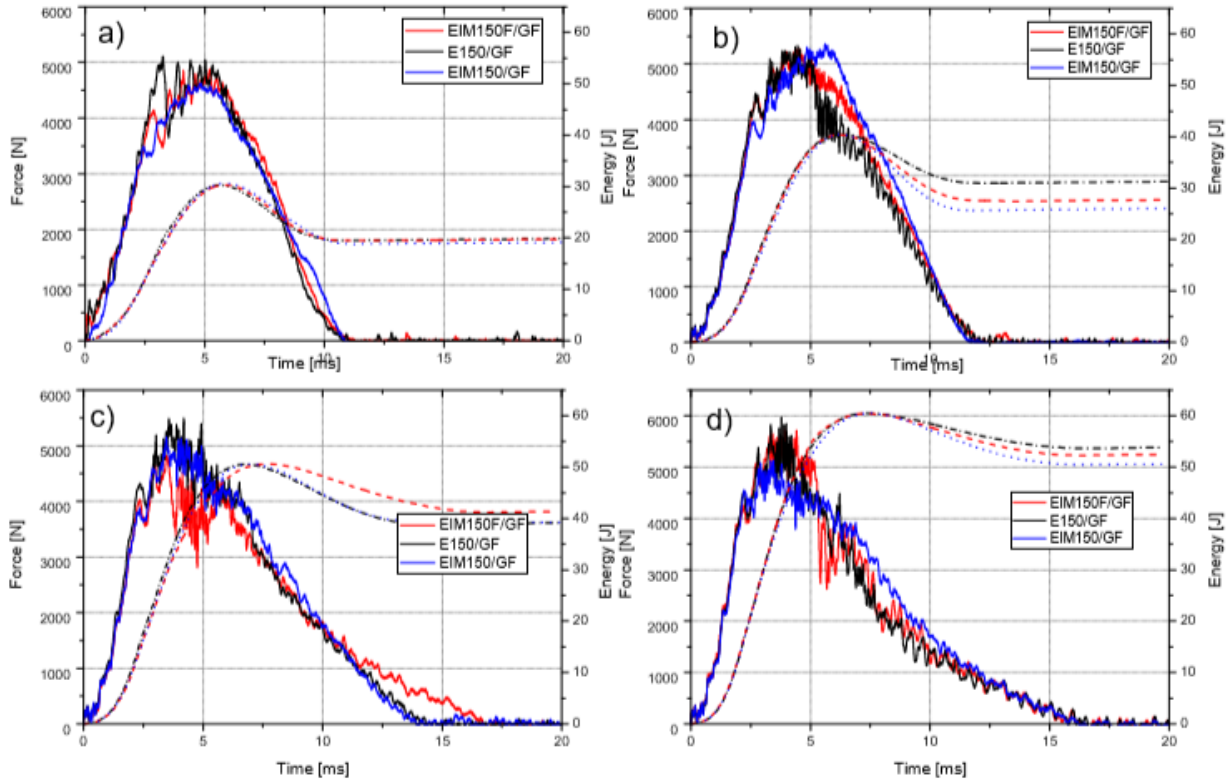


Figure 17: Force-displacement and energy-time curves, showing the effect of copolymers, at impact energies of: (a) 30 J; (b) 40 J; (c) 50 J; (d) 60 J.

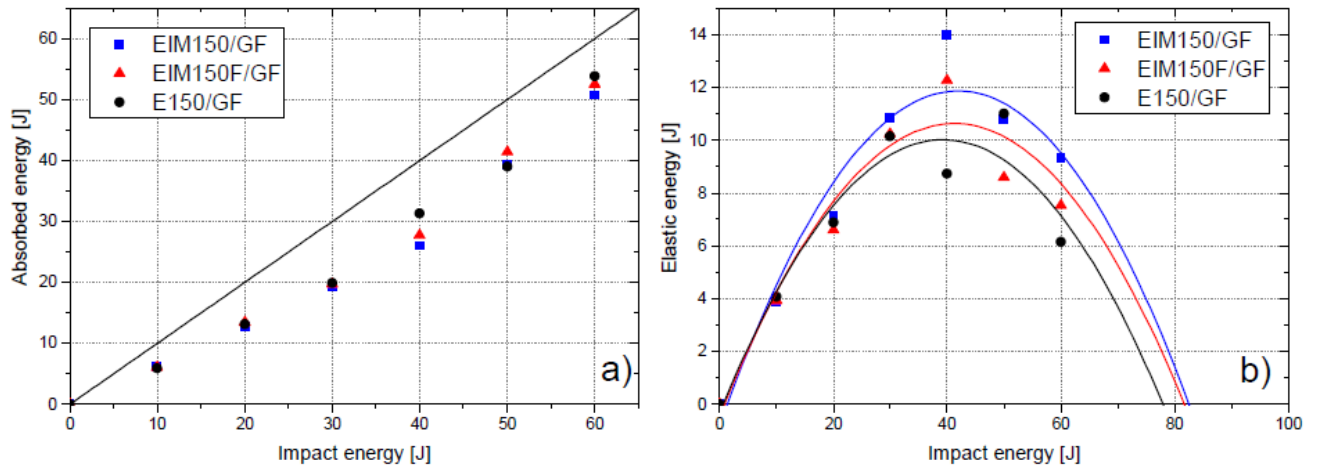


Figure 18: Effect of copolymers on the penetration threshold of glass fiber reinforced acrylic thermoplastic composites at 20 °C. Curves of: (a) absorbed energy versus impact energy, (b) elastic energy versus impact energy.

Table captions:*Table 1: Materials and manufacturing processes*

Material	Nomenclature	Used process	Type of modifier
Glass fibers/Epoxy	Epoxy/GF	Infusion process	
Glass fibers/Polyester	Polyester/GF	Infusion process	
Glass fibers/Elium-Acrylic	E150/GF	Infusion process	
Glass fibers/(Elium-Acrylic+10wt% of Nanostreh tri-blocks copolymers)	EIM150F/GF	Infusion process	Acrylic rubber which is grafted to the PMMA matrix during the polymerization of MMA and dispersed at a nano-scale
Glass fibers/(Elium-Acrylic+10wt% of Acrylonitrile butadiene styrene copolymer (ABS))	EIM150/GF	Infusion process	Acrylonitrile butadiene styrene grafted to the PMMA matrix during the polymerization of MMA and dispersed at a nano-scale